

E. A. Johnson · G. R. Rossman

## An infrared and $^1\text{H}$ MAS NMR investigation of strong hydrogen bonding in ussingite, $\text{Na}_2\text{AlSi}_3\text{O}_8(\text{OH})$

Received: 22 April 2003 / Accepted: 16 October 2003

**Abstract** The mineral ussingite,  $\text{Na}_2\text{AlSi}_3\text{O}_8(\text{OH})$ , an “interrupted” tectosilicate, has strong hydrogen bonding between OH and the other nonbridging oxygen atom in the structure. Infrared spectra contain a strongly polarized, very broad OH-stretching band with an ill-defined maximum between 1500 and 1800  $\text{cm}^{-1}$ , and a possible OH librational bending mode at 1295  $\text{cm}^{-1}$ . The IR spectra confirm the orientation of the OH vector within the triclinic unit cell as determined from X-ray refinement (Rossi et al. 1974). There are three distinct bands in the  $^1\text{H}$  NMR spectrum of ussingite: a predominant band at 13.5 ppm (TMS) representing 90% of the structural hydrogen, a second band at 15.9 ppm corresponding to 8% of the protons, and a third band at 11.0 ppm accounting for the remaining 2% of structural hydrogen. From the correlation between hydrogen bond length and  $^1\text{H}$  NMR chemical shift (Sternberg and Brunner 1994), the predominant hydrogen bond length ( $\text{H}\cdots\text{O}$ ) was calculated to be 1.49 Å, in comparison to the hydrogen bond length determined from X-ray refinement (1.54 Å). The population of protons at 15.9 ppm is consistent with 5–8% Al–Si disorder. Although the ussingite crystal structure and composition are similar to those of low albite, the bonding environment of OH in

low albite and other feldspars, as characterized through IR and  $^1\text{H}$  NMR, is fundamentally different from the strong hydrogen bonding found in ussingite.

**Keywords** Infrared spectroscopy · NMR spectroscopy · Ussingite · Low albite · Hydrogen

### Introduction

Ussingite,  $\text{Na}_2\text{AlSi}_3\text{O}_8(\text{OH})$ , is a very rare mineral first identified by Böggild (1914) that occurs in extremely basic, silica-poor sodalite syenites (hyperagpaitic rocks) (Sørensen 1997). Ussingite formed as a late-stage hydrothermal pegmatite mineral in the Ilímaussaq intrusive complex in southwest Greenland (Engell et al. 1971) and the Lovozero and Khibina complexes of the Kola peninsula (Ilyukhin and Semenov 1959). It is also found in sodalite xenoliths in the Mont Saint-Hilaire, Canada, alkalic gabbro–syenite complex (Mandarino and Anderson 1989).

The crystallographic structure of ussingite was determined by Rossi et al. (1974). Ussingite has an “interrupted” aluminosilicate framework structure, in which seven of the nine oxygen atoms are bridging oxygens linking the Al and Si tetrahedra in four-, six-, and eight-fold rings. The remaining two oxygen atoms [O(2) and O(8)] are nonbridging and participate in hydrogen bonding (Fig. 1). The O(8)–H, O(2)–H, and O(2)–O(8) distances were determined from structural refinement of the X-ray data to be 0.97, 1.54, and 2.507 Å, respectively. The hydrogen bonding in ussingite is characterized as strong, since the O(2)–O(8) distance is significantly shorter than the sum of the van der Waals radii of two oxygen atoms (about 3.0 Å) (Emsley 1981). As is typical for strongly hydrogen-bonded systems, the O(2)–H–O(8) angle is nearly linear (171°) (Rossi et al. 1974).

The Al in ussingite is almost completely ordered into the T(1) tetrahedron, one of four tetrahedral sites in the structure (Rossi et al. 1974). However, Ribbe (1974) found a better agreement between observed and calcu-

E.A. Johnson (✉)  
Division of Geological and Planetary Sciences,  
MS 100-23, California Institute of Technology,  
Pasadena, CA 91125, USA

G.R. Rossman  
Division of Geological and Planetary Sciences,  
MS 100-23, California Institute of Technology,  
Pasadena, CA 91125, USA

*Present address:* E.A. Johnson  
Smithsonian Institution,  
Department of Mineral Sciences,  
National Museum of Natural History,  
MRC 0119,  
Washington, DC 20119, USA  
e-mail: johnson.elizabeth@nmnh.si.edu  
Tel.: 202-786-2555  
Fax: 202-357-2476

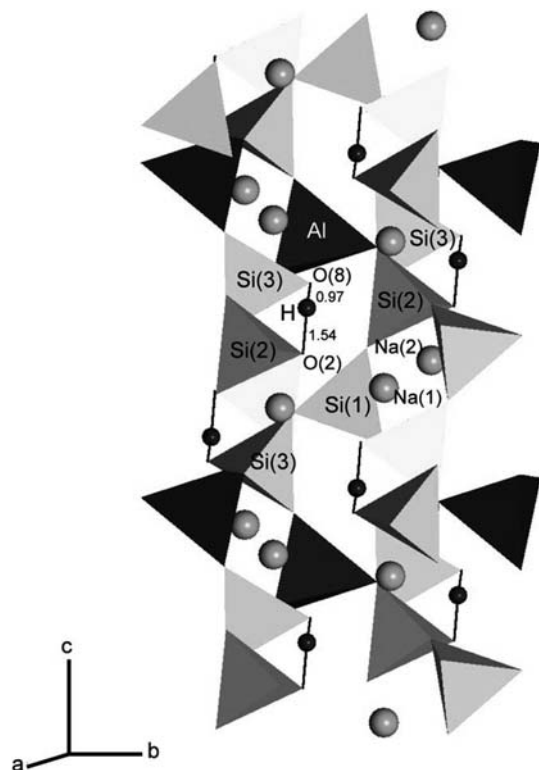


Fig. 1 The crystal structure of ussingite projected onto (100)

lated T–O distances for ussingite when 5% of the Al was transferred from T(1) to T(3). Ussingite is triclinic, but it exhibits a pseudomonoclinic symmetry (Rossi et al. 1974). The complete Al–Si ordering and the asymmetric nature of the O–H···O bonding are the causes of the triclinic symmetry.

Previous workers have investigated some of the physical properties, the crystallographic structure, and chemistry of ussingite. A  $^{29}\text{Si}$  nuclear magnetic resonance (NMR) and  $^{29}\text{Si}$ – $^1\text{H}$  cross-polarization (CP) NMR study confirmed the assignment of Si to three tetrahedral sites and provided additional constraints on Si–H distances in the ussingite structure (Oglesby and Stebbins 2000). Thermal gravimetric analysis showed that ussingite is dehydrated over a temperature range of 500 to 650 °C (Ilyukhin and Semenov 1959). Several sets of chemical analyses report that ussingite largely contains stoichiometric Na, Al, Si, and H (Böggild 1914), with some samples containing minor amounts of K, Ca, Fe, Mn, S, and Cl (Ilyukhin and Semenov 1959; Povarennykh et al. 1970).

However, the OH in ussingite has not previously been characterized with IR or  $^1\text{H}$  NMR spectroscopy. Both of these techniques can provide important constraints on the nature of hydrogen bonding. Correlations have been established between hydrogen bond length and  $^1\text{H}$  NMR chemical shift (Jeffrey and Yeon 1986; Sternberg and Brunner 1994), as well as between the IR OH-stretching frequency and O–H···O distance (Nakamoto et al. 1955; Libowitzky 1999) for minerals and solid hydrates.

The crystallographic orientation of the OH vector can be determined accurately with single-crystal polarized IR spectroscopy. Magic-angle spinning (MAS) NMR reduces the band width of the proton signal in solids, so that it is possible to resolve proton populations that experience slightly different hydrogen-bonding environments.

As discussed in Ribbe (1974) and Rossi et al. (1974), there are striking similarities between the structures of low albite and ussingite. Both structures have complete or nearly complete Al–Si ordering in tetrahedra that form four-, six-, and eight-fold rings, and in both structures the Na atoms are irregularly coordinated (with coordination numbers of five and six in ussingite, and five in low albite) (Rossi et al. 1974; Downs et al. 1996). In fact, an equation derived from structural data of sodic plagioclases used to quantitatively describe the variation in T–O bond lengths in these minerals produces excellent estimates of the Al–O, Si–O, and Si–(OH) bond distances in ussingite (Ribbe 1974).

There are two main purposes for conducting this study. The first is to determine if the stoichiometric OH observed in ussingite (2.98 wt%  $\text{H}_2\text{O}$ ) can be used as a structural model for the small quantities (0–0.051 wt%  $\text{H}_2\text{O}$ ) of structural OH that are incorporated into low albite as well as other plagioclase feldspars, sanidine, and anorthoclase (Hofmeister and Rossman 1985a, b; Hofmeister and Rossman 1986; Johnson and Rossman 2003). The mechanism for how OH is incorporated into the feldspar structures is unknown, so a comparison of the IR and  $^1\text{H}$  NMR spectra of OH in feldspars (Johnson and Rossman 2003) and the OH in ussingite will provide important constraints on the possible bonding environments of OH in feldspars. The second reason for this study is that there have been few IR investigations of strong and very strong hydrogen bonding in minerals, such as serandite and pectolite (Hammer et al. 1998), and mozartite (Nyfeler et al. 1997). A complete study of the IR spectra of ussingite will increase knowledge of the characteristics (energy, band shape, polarization, and symmetry) of strong hydrogen bonds in minerals.

## Experimental

The ussingite used in this study is from the Ilímaussaq complex, Greenland (sample GRR1967). It occurs in a white, transparent to translucent granular aggregate. Single crystals are less than 100  $\mu\text{m}$  to several millimeters across. Mineral identification was confirmed with powder X-ray diffraction.

Oriented, polished slabs of single crystals were prepared for infrared spectroscopic measurements using cleavage and twin planes. Because of the granular nature of the sample, no crystal faces were visible. Three cleavages,  $c\{001\}$ ,  $m\{110\}$ , and  $M\{110\}$ , were originally reported for ussingite (Böggild 1914). In the present study the triclinic unit cell of Rossi et al. (1974) was used ( $a = 7.256$ ,  $b = 7.686$ ,  $c = 8.683$  Å,  $\alpha = 90^\circ 45'$ ,  $\beta = 99^\circ 45'$ ,  $\gamma = 122^\circ 29'$ ), and in these coordinates the cleavages are:  $c\{100\}$ ,  $m\{011\}$ , and  $M\{1\bar{1}\bar{1}\}$ . A polished slab was prepared parallel to the  $\{100\}$  cleavage to obtain polarized IR spectra with  $E\parallel b$  and  $E\parallel c$ . The  $b$  and  $c$  axes are nearly perpendicular to each other ( $\alpha = 90^\circ 45'$ ) (Rossi et al. 1974), and the angle between the normal to (010) and the principal optical direction  $Y$  is  $5$ – $6^\circ$  (Böggild 1914), which, in addition to cleavage planes, made

it possible to locate the  $b$  and  $c$  axes within the polished slab. Twinning occurs parallel to  $\{010\}$ , and grains lying on this surface produce a slightly off-center flash figure. The principal optical direction  $Z$  (the acute bisectrix) is about  $33^\circ$  from the vector normal to  $(100)$  in the  $\{010\}$  plane (Böggild 1914). Thus, it was possible to obtain a polarized spectrum with  $E||a$  on a polished slab parallel to  $(010)$ . It was necessary to fabricate polished slabs that were as thin as possible, since ussingite has a relatively high OH concentration (2.98 wt%  $\text{H}_2\text{O}$ ), and because the OH bands overlap the very intense silicate modes. Slabs were prepared with  $\text{Al}_2\text{O}_3$  and diamond films. The grain was mounted on a circular thin-section slide with Crystalbond thermal adhesive, and after preparation, the adhesive was dissolved in acetone to produce an unsupported, slightly wedge-shaped slab for IR work. The thickness of the portion of each slab used to obtain IR spectra was determined using the birefringence colors obtained under crossed polars (refractive indices  $\alpha = 1.504$ ,  $\beta = 1.508$ ,  $\gamma = 1.545$ ) (Böggild 1914). The final polished slabs were  $17\ \mu\text{m}$  thick  $(010)$  and  $15\ \mu\text{m}$  thick  $(100)$ .

Polarized infrared spectra were obtained in the  $400\text{--}5000\ \text{cm}^{-1}$  region using a Spectra-Tech Continuum microscope accessory with a Nicolet Magna 860 FTIR spectrometer at  $4\ \text{cm}^{-1}$  resolution, an extended-range KBr beamsplitter, Au wire grid on AgBr polarizer, and MCT-B detector. Each spectrum was averaged over 512 scans, using a  $50\text{--}100\text{-}\mu\text{m}$ -square aperture.

$^1\text{H}$  MAS NMR spectra were recorded on a Bruker DSX 500 MHz spectrometer and a Bruker Avance 200 MHz spectrometer at the solid-state NMR facility in the Department of Chemical Engineering at Caltech. A  $4\text{-}\mu\text{s}\ 90^\circ\text{--}8\text{-}\mu\text{s}\ 180^\circ$  pulse depth sequence (program written by Sonjong Hwang; Cory and Ritchey 1988) was used to minimize probe background for most spectra. Tetraakis-(trimethylsilyl)silane (TKTMS) was used as a primary chemical shift ( $\delta$ ) reference, but final spectra are referenced to tetramethylsilane (TMS), using the relationship  $\delta(\text{TMS}) = \delta(\text{TKTMS}) + 0.247\ \text{ppm}$  (Hayashi and Hayamizu 1991). Saturation-recovery experiments were used to determine a spin-lattice relaxation time  $T_1$  of about 100 s for all of the structural hydrogen environments in ussingite. The recycle delay time was set at 510 s, or roughly five times  $T_1$ . Variable temperature experiments were conducted between 178 and 373 K. Dry nitrogen from a high-pressure liquid nitrogen tank was used for cooling and spinning the samples.

## Results

The polarized infrared spectra of ussingite are shown in Fig. 2. In each spectrum, the absorption bands of the silicate modes ( $1200\text{--}600\ \text{cm}^{-1}$ ) are off-scale (absorbance is greater than 2.0). The  $E||b$  spectrum is characterized by a flat background in the  $3500\text{--}1300\ \text{cm}^{-1}$  region, with a small, broad absorbance band at about  $1700\ \text{cm}^{-1}$  and a sharper, more intense band at  $1295\ \text{cm}^{-1}$ . The  $E||c$  spectrum lacks the  $1295\ \text{cm}^{-1}$  band, but has a very broad and intense band that begins at around  $3000\ \text{cm}^{-1}$  and continues under the silicate modes to less than  $800\ \text{cm}^{-1}$ . This broad band is interrupted by features at  $2500$ ,  $2200$ , and  $1300\ \text{cm}^{-1}$  that resemble notches or inverse bands that cut into the absorption. It is difficult to determine the exact energy of the maximum absorbance of this band due to its width and due to the interference of the silicate modes and inverse bands. However, the maximum absorbance most likely occurs between  $1500$  and  $1800\ \text{cm}^{-1}$ , since the intensity of this broad band in the minimum at  $850\ \text{cm}^{-1}$  is roughly equivalent to that at  $3000\ \text{cm}^{-1}$ , after subtraction of estimated absorbance due to the silicate modes. Finally, the spectrum taken with  $E||a$  also contains a weak component of this very broad band, although it is not as

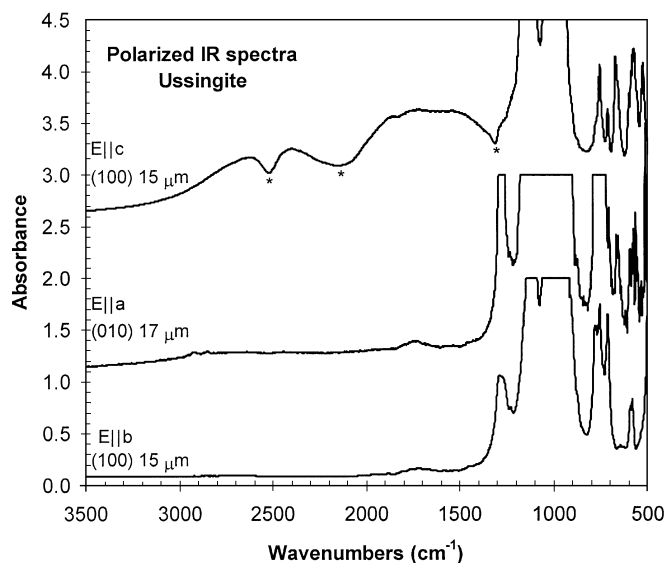


**Fig. 2** Polarized single-crystal infrared spectra of ussingite. The asterisks mark the “inverse” Fermi resonances superimposed on the broad OH band ( $3000\text{--}800\ \text{cm}^{-1}$ ). Some silicate bands are off-scale and have been truncated. The spectra have been offset vertically for comparison

intense and lacks the prominent notches seen in  $E||c$ . The narrow band at  $1298\ \text{cm}^{-1}$  is most intense in the  $E||a$  spectrum.

There are three distinct bands present in the  $^1\text{H}$  MAS NMR spectra of ussingite. The NMR spectra taken at 6 and 12 kHz magic angle spinning speeds are shown in Fig. 3a. Spinning sidebands occur at intervals of the spinning speed on either side of the primary bands. There is one predominant band in the spectrum at  $\delta = 13.9\ \text{ppm}$ , which (along with its spinning sidebands) accounts for 90% of the total band area and  $^1\text{H}$  in the crystal structure. The other two primary bands are at  $\delta = 15.9\ \text{ppm}$  and  $\delta = 11.0\ \text{ppm}$ , and represent about 8% and 2% of total structural hydrogen, respectively. The band at 4 ppm is due to adsorbed water on the sample and materials in the NMR probe (Johnson and Rossman 2003). The center bands of  $^1\text{H}$  MAS spectra obtained using different magnetic field strengths and pulse sequences are presented in Fig. 3b. The three distinct  $^1\text{H}$  bands are present in the spectra regardless of field strength (200 and 500 MHz) and pulse sequence (a depth sequence versus a single pulse), although the fine structure of the band at  $15.9\ \text{ppm}$  is apparently an artifact caused by the depth-pulse sequence since it is not present in the single-pulse experiment. The shapes, positions, and proportions of all three bands in the ussingite  $^1\text{H}$  NMR spectrum remain constant over a range of temperatures ( $178\text{--}373\ \text{K}$ ).

## Discussion

### IR spectroscopy

The energy of maximum absorption and width of the very broad band in the  $E||c$  and  $E||a$  IR spectra in Fig. 2 are

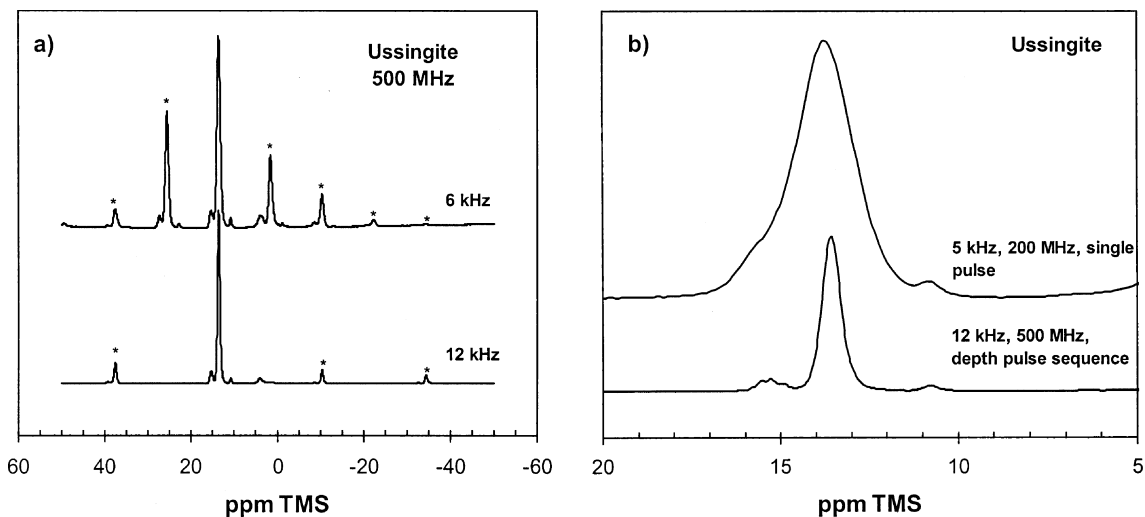


**Fig. 3a, b**  $^1\text{H}$  MAS NMR spectra of ussingite. **a** Spectra obtained on a 500 MHz magnet at 6 kHz and 12 kHz magic-angle spinning speeds, showing the main bands and spinning sidebands (marked with *asterisks*). The band at 4 ppm is due to adsorbed water and probe materials. **b** Expanded view of the three center bands of ussingite spectra taken on a 500 MHz magnet using a depth pulse sequence and a 200-MHz magnet using a single pulse

characteristic of OH bands in other silicate minerals that have strong or very strong hydrogen bonding. For example, pectolite,  $\text{NaCa}_2[\text{Si}_3\text{O}_8(\text{OH})]$  and serandite,  $\text{NaMn}_2[\text{Si}_3\text{O}_8(\text{OH})]$ , have O–H $\cdots$ O distances of 2.45 to 2.48 Å, and have OH-stretching bands that are centered at approximately  $1000\text{ cm}^{-1}$  and span a region from greater than  $3000\text{ cm}^{-1}$  to less than  $600\text{ cm}^{-1}$  (Hammer et al. 1998). Similarly, the IR spectrum of mozartite,  $\text{CaMn}^{3+}\text{O}[\text{SiO}_3\text{OH}]$ , has an extremely broad OH-stretching band with a maximum at  $1300\text{--}1700\text{ cm}^{-1}$ , and a corresponding O–H $\cdots$ O distance of 2.501 Å (Nyfeler et al. 1997). The unusual notches or inverse absorbance features that interrupt the OH-stretching band in the ussingite spectra are also present in the IR spectra of mozartite, pectolite, and serandite (Nyfeler et al. 1997; Hammer et al. 1998). These features are called Fermi (or Fano) resonances, and are caused by the interaction of the broad OH stretching with the OH-bending librations (Hadži and Bratos 1976; Emsley 1981; Struzhkin et al. 1997). The unusual structure of the most intense region of the OH band (a central maximum with weaker submaxima) is also seen in hydrogen-bonded complexes of ethers with hydrogen halides and is most likely due to sum and difference modes of the OH stretch and a low-energy stretching mode in the structure (Hadži and Bratos 1976).

The broad OH-stretching band is very strongly polarized. This very strong polarization of the OH-stretching frequency is consistent with the strong directionality of the OH vector in the triclinic symmetry of ussingite. The  $E||c$  spectrum has very strong OH absorption (Fig. 2), whereas the  $E||b$  spectrum has little or no OH stretch absorption, consistent with the alignment of the OH vector in the crystal structure (Fig. 1). In the (010) plane, the OH vector is aligned with the

principal optical direction  $Z$ , which is not aligned with the crystallographic axes. This is the reason for the intermediate OH stretch absorption in the  $E||a$  spectrum.

It is known that the OH-stretching frequency is related to the strength of hydrogen bonding for many materials. More specifically, the OH-stretching frequency decreases with decreasing length of hydrogen bonding, due to a combination of a decrease in the bond strength (and force constant) of the hydroxyl group and an increase in vibrational anharmonicity (Lutz 1988). A number of experimental studies have quantified the relationship between hydrogen bonding and IR frequency in organic and inorganic compounds, including minerals, and discuss the deviations from this correlation due to the effects of nonlinear and bifurcated geometries and proton dynamics (e.g., Nakamoto et al. 1955; Libowitzky 1999), as well as the effects of cation substitution into crystallographic sites adjacent to OH (Skogby and Rossman 1991). The precise energy of the maximum OH stretch intensity of ussingite is not tightly constrained, but occurs between  $1500$  and  $1800\text{ cm}^{-1}$ . Using the correlation between OH-stretching frequency and O–H $\cdots$ O distance given in Libowitzky (1999)  $\nu(\text{cm}^{-1}) = 3592 - 304 \times 10^9 \exp[-d(\text{O}-\text{H}\cdots\text{O})/0.1321]$ , the O–H $\cdots$ O distance in ussingite is calculated to be 2.48–2.50 Å. This agrees well with the O(2)–O(8) distance of 2.507 Å determined by least-squares refinement (Rossi et al. 1974).

The band at  $1295\text{ cm}^{-1}$  in the  $E||a$  and  $E||b$  spectra of ussingite may be an OH librational bending mode or a silicate mode or overtone. There are three reasons for concluding that this band is an OH-bending mode. The OH-bending mode is expected to be infrared active in a direction perpendicular to the OH vector, and the  $1295\text{ cm}^{-1}$  band is absent in the  $E||c$  spectrum but present in the  $E||b$  and  $E||a$  spectra. Other minerals with strongly hydrogen-bonded OH groups also have OH-bending modes at energies higher than the fundamental silicate modes (serandite at  $1386\text{ cm}^{-1}$ , pectolite at  $1396\text{ cm}^{-1}$ ; Hammer et al. 1998). Finally, the highest-energy Fermi resonance occurs at

2525  $\text{cm}^{-1}$ , which is approximately twice the frequency of the 1295  $\text{cm}^{-1}$  mode. The origin of the other two Fermi resonances is unknown.

### $^1\text{H}$ MAS NMR spectroscopy

The  $^1\text{H}$  NMR chemical shift is largely determined by O–H bond polarization, which is dominated by hydrogen bonding to the neighboring oxygen (Sternberg and Brunner 1994). Short hydrogen-bonding distances increase bond polarization and thus also increase the proton chemical shift relative to protons that experience weak hydrogen bonding. Since ussingite has only one hydrogen site with a single hydrogen-bonding distance ( $\text{H}\cdots\text{O}$ ), only one band is expected in the  $^1\text{H}$  NMR data, and in fact most of the protons (90%) constitute a single band at 13.9 ppm. Using the correlation between inverse hydrogen bond length  $r\text{H}\cdots\text{O}^{-1}$  and isotropic chemical shift  $\delta_{\text{H}}$  determined by Sternberg and Brunner (1994) [ $\delta_{\text{H}}$  (ppm) =  $4.65/r\text{H}\cdots\text{O} - 17.4$ ], the band at 13.9 ppm corresponds to an  $\text{H}\cdots\text{O}$  bond length of 1.49 Å. This distance is slightly shorter but within 5% of the  $\text{H}\cdots\text{O}$  distance determined from X-ray refinement (1.54 Å) (Rossi et al. 1974).

There are two additional NMR bands (about 10% of the protons) that are not accounted for with this model. The Al in ussingite was originally determined to be completely ordered in the T(1) site, with Si filling the remaining three tetrahedral sites, including the T(4) site attached to the O(8) hydroxyl-forming oxygen atom and the T(3) site coordinated by the O(2) hydrogen-bonding oxygen atom (Rossi et al. 1974). However, Ribbe (1974) found that the mean T(1)–O distance in ussingite was significantly shorter (0.01–0.013 Å) than the mean Al–O distance in low albite. Ribbe (1974) concluded that about 5% of the Al was in the T(3) site rather than the T(1) site. Since Al–O bonds are longer than the Si–O bonds, in a local bonding environment where Al is substituted for the Si in the T(3) site, the increased T(3)–O bond length would result in a shorter hydrogen bond length and a higher  $^1\text{H}$  NMR chemical shift value. The relative underbonding of the O(2) attached to Al rather than Si would also be expected to increase hydrogen bonding. To quantify this expected shift in  $\delta$ , the difference between the mean Al–O bond distance for the T(1) site (1.734 Å) and the Si–O(2) bond distance for the T(3) site (1.584 Å) (Rossi et al. 1974) was calculated to be 0.15 Å. Shortening the  $\text{H}\cdots\text{O}$  distance by this amount results in a hydrogen bond length of 1.39 Å and a predicted chemical shift of 16.0 ppm. This value of  $\delta$  agrees well with the observed  $\delta = 15.9$  ppm of the band in the ussingite  $^1\text{H}$  NMR spectrum corresponding to 8% of the total hydrogen concentration. This calculation assumes that the T(3) cation, O(8), H, and O(2) are all colinear. If the fact that the T(3)–O(8)–H angle is about  $138^\circ$  rather than  $180^\circ$  is accounted for in this calculation, then the chemical shift for a hydrogen adjacent to Al in

the T(3) site is determined to be 15.3 ppm, assuming an O–H $\cdots$ O distance of 2.5 Å from the IR data, an OH distance of 0.97 Å from X-ray refinement (Rossi et al. 1974), and allowing the T(3)–O(8)–H angle to change upon lengthening of the T(3)–O(8) distance by 0.15 Å. The  $^1\text{H}$  NMR spectrum therefore provides an independent confirmation of minor amounts of Al–Si disorder between T(1) and T(3) in ussingite.

The band at  $\delta = 11.0$  ppm represents about 2% of the total hydrogen atoms, or about 0.06 wt%  $\text{H}_2\text{O}$ . The  $\text{H}\cdots\text{O}$  bond distance calculated for this value of  $\delta$  is 1.64 Å. The origin of this band is unknown, but it is possible that local distortion of the crystal structure due to the substitution of  $\text{Ca}^{2+}$  for  $2\text{Na}^+$ , for example, could result in longer hydrogen bonding distances and lower the chemical shift value. Alternatively, small amounts of other mineral impurities in the ussingite sample could be responsible for this  $^1\text{H}$  NMR band, although an investigation of the sample with optical microscopy and Raman spectroscopy revealed only alteration products, most likely zeolites, forming distinct coatings on the outside surface of the hand sample.

The lack of temperature dependence of the band positions and shapes in the  $^1\text{H}$  NMR spectrum and the long spin-lattice relaxation time (100 s) indicate there is little or no dynamic chemical motion involving the protons in ussingite.

### Criteria for strong hydrogen bonding

The criteria for classifying hydrogen bonds as strong or weak are summarized in Emsley (1981), and include considerations of bond length, O–H $\cdots$ O bond symmetry, infrared OH and OD stretch modes, NMR chemical shift, and bond energy. As mentioned above, the O–H $\cdots$ O distance (as determined by X-ray refinement and now IR spectroscopy) in ussingite characterizes it as a material with strong hydrogen bonding. The large downfield  $^1\text{H}$  NMR chemical shift and broad IR OH-stretching band with a maximum of 1500–1800  $\text{cm}^{-1}$  are also consistent with the definition of strong hydrogen bonding.

In general, strong hydrogen bonds tend to be linear, i.e., the O–H $\cdots$ O angle is about  $180^\circ$  (Emsley 1981), and indeed this angle is  $171^\circ$  in ussingite (Rossi et al. 1974). For strong hydrogen bonds, it has been suggested that the hydrogen atom is symmetrically centered between the oxygen atoms (Emsley 1981), but the data in this study point to an asymmetric bonding environment. The  $\text{H}\cdots\text{O}$  distance for ussingite constrained by  $^1\text{H}$  NMR data is significantly longer than half of the O–H $\cdots$ O distance determined with IR spectroscopy. There are many recently reported examples of minerals with strong hydrogen bonding exhibiting asymmetric O–H $\cdots$ O bonding (Beran and Libowitzky 1999), so it is concluded that ussingite is well characterized as a material with strong hydrogen bonding.

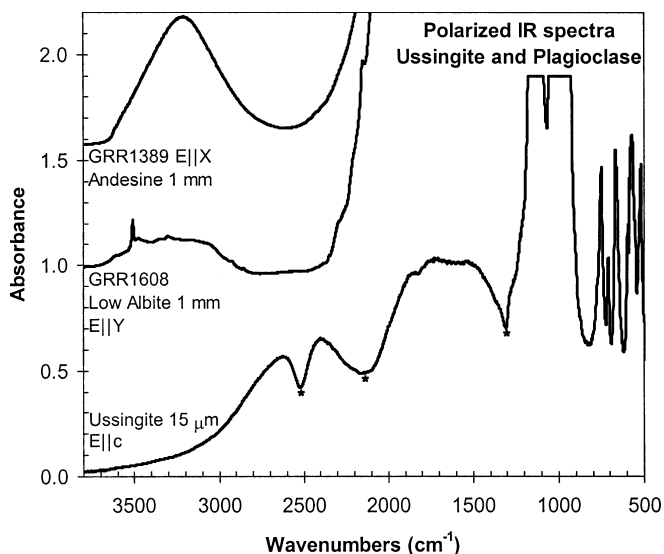


**Fig. 4** Comparison of the polarized IR spectra of low albite, andesine, and ussingite, indicating the difference in hydrogen-bonding environments between feldspars and ussingite

#### Comparison of OH in ussingite to OH in feldspars

The nature of OH in low albite or other plagioclase feldspars is apparently very different from that of the OH in ussingite, despite similarities in their respective crystal structures. This can be seen in the polarized IR spectra of low albite, andesine, and ussingite in Fig. 4. The silicate modes in the thick feldspar samples are off-scale below  $2300\text{ cm}^{-1}$ , but it is still possible to observe the differences between the feldspar and ussingite spectra in the  $3000\text{--}3700\text{ cm}^{-1}$  region. Low albite is characterized by very sharp OH bands around  $3500\text{ cm}^{-1}$ , a broad underlying fluid inclusion band at about  $3450\text{ cm}^{-1}$ , and a broad OH band around  $3050\text{ cm}^{-1}$  (Johnson and Rossman 2003). Andesine (and other plagioclase and alkali feldspars) have broader OH bands in the  $3000\text{--}3500\text{ cm}^{-1}$  region, and no Fermi resonances are visible in the spectrum. The  $^1\text{H}$  NMR chemical shift of OH in feldspars (4–6 ppm) is much smaller than the  $\delta$  for OH in ussingite (11–15.9 ppm), and there are no detectable bands in the 11–15.9-ppm region of feldspar  $^1\text{H}$  NMR spectra (Johnson and Rossman 2003). Therefore, a maximum of about 10–20 ppm  $\text{H}_2\text{O}$  could be present as strongly hydrogen-bonded OH in these feldspars. Unlike the OH in ussingite, the OH in feldspars is therefore not strongly hydrogen-bonded.

**Acknowledgements** E.A.J. thanks Sonjong Hwang for assistance with the  $^1\text{H}$  NMR measurements. This research was supported by National Science Foundation grants EAR-0125767 and EAR-9804871. The sample of ussingite was donated by D.S. Barker (UT Austin). The authors thank E. Libowitzky and an anonymous reviewer for improving the manuscript. This is contribution number 8959 of the Division of Geological and Planetary Sciences of the California Institute of Technology.

#### References

- Beran A, Libowitzky E (1999) IR spectroscopy and hydrogen bonding in minerals. In: Wright K, Catlow R (eds) *Microscopic properties and processes in minerals*. Kluwer Academic, The Netherlands, pp 493–508
- Böggild OB (1914) Ussingit, ein neues Mineral von Kangerdluar-suk. *Z Kristallogr* 54: 120–126
- Cory DG, Ritchey WM (1988) Suppression of signals from the probe in Bloch decay spectra. *J Magn Reson* 80: 128–132
- Downs RT, Andalman A, Hudacsko M (1996) The coordination numbers of Na and K atoms in low albite and microcline as determined from a procrystal electron-density distribution. *Am Mineral* 81: 1344–1349
- Emsley J (1981) Very strong hydrogen bonding. *Chem Soc Rev* 9: 91–124
- Engell J, Hansen J, Jensen M, Kunzendorf H, Lovborg L (1971) Beryllium mineralization in the Ilimaussaq intrusion, South Greenland, with description of a field beryllometer and chemical methods. *Grønlands Geologiske Undersøgelse Rapport* 33: 1–40
- Hadži D, Bratos S (1976) Vibrational spectroscopy of the hydrogen bond. In: Schuster P et al. (eds) *The hydrogen bond — recent developments in theory and experiments*. North Holland, Amsterdam, pp 567–611
- Hammer VMF, Libowitzky E, Rossman GR (1998) Single-crystal IR spectroscopy of very strong hydrogen bonds in pectolite,  $\text{NaCa}_2[\text{Si}_3\text{O}_8(\text{OH})]$ , and serandite,  $\text{NaMn}_2[\text{Si}_3\text{O}_8(\text{OH})]$ . *Am Mineral* 83: 569–576
- Hayashi S, Hayamizu K (1991) Chemical shift standards in high-resolution solid-state NMR (I)  $^{13}\text{C}$ ,  $^{29}\text{Si}$ , and  $^1\text{H}$  nuclei. *Bull Chem Soc Jpn* 64: 685–687
- Hofmeister AM, Rossman GR (1985a) A spectroscopic study of irradiation coloring of amazonite: structurally hydrous, Pb-bearing feldspar. *Am Mineral* 70: 794–804
- Hofmeister AM, Rossman GR (1985b) A model for the irradiative coloration of smoky feldspar and the inhibiting influence of water. *Phys Chem Miner* 12: 324–332
- Hofmeister AM, Rossman GR (1986) A spectroscopic study of blue radiation coloring in plagioclase. *Am Mineral* 71: 95–98
- Ilyukhin VV, Semenov YI (1959) New data on ussingite. *Dokl Earth Sci* 129: 1176–1178
- Jeffrey GA, Yeon Y (1986) The correlation between hydrogen-bond lengths and proton chemical shifts in crystals. *Acta Crystallogr (B) Struct Sci* 42: 410–413
- Johnson EA, Rossman GR (2003) The concentration and speciation of hydrogen in feldspars using FTIR and  $^1\text{H}$  MAS NMR spectroscopy. *Am Mineral* 88: 901–911
- Libowitzky E (1999) Correlation of O–H-stretching frequencies and O–H...O hydrogen bond lengths in minerals. *Monatsh Chem* 130: 1047–1059
- Lutz HD (1988) Bonding and structure of water molecules in solid hydrates—correlation of spectroscopic and structural data. *Structure Bonding* 69: 97–125
- Mandarino JA, Anderson V (1989) *Monteregian treasures: the minerals of Mont Saint-Hilaire, Quebec*. Cambridge University Press, Cambridge, p 207
- Nakamoto K, Margoshes M, Rundle RE (1955) Stretching frequencies as a function of distances in hydrogen bonds. *J Am Chem Soc* 77: 6480–6486
- Nyfelner D, Hoffmann C, Armbruster T, Kunz M, Libowitzky E (1997) Orthorhombic Jahn-Teller distortion and Si–OH in moztartite,  $\text{CaMn}^{3+}\text{O}[\text{Si}_3\text{O}_7\text{OH}]$ : a single-crystal X-ray, FTIR, and structure modeling study. *Am Mineral* 82: 841–848
- Oglesby JV, Stebbins JF (2000)  $^{29}\text{Si}$  CPMAS NMR investigations of silanol-group minerals and hydrous aluminosilicate glasses. *Am Mineral* 85: 722–731
- Povarennykh AS, Platonov AN, Belichenko VP (1970) On the colour of ussingite from the Ilimaussaq (South Greenland) and

- Lovozero (Kola Peninsula) alkaline intrusions. *Bull Geol Soc Denmark* 20: 20–26
- Ribbe PH (1974) A comparison of bonding effects in ussingite and low albite. *Am Mineral* 59: 341–344
- Rossi G, Tazzoli V, Ungaretti L (1974) The crystal structure of ussingite. *Am Mineral* 59: 335–340
- Skogby H, Rossman GR (1991) The intensity of amphibole OH bands in the infrared absorption spectrum. *Phys Chem Miner* 18: 64–68
- Sørensen H (1997) The agpaitic rocks—an overview. *Mineral Mag* 61: 485–498
- Sternberg U, Brunner E (1994) The influence of short-range geometry on the chemical shift of protons in hydrogen bonds. *J Mag Reson, Ser A* 108: 142–150
- Struzhkin VV, Goncharov AF, Hemley RJ, Mao HK (1997) Cascading Fermi resonances and the soft mode in dense ice. *Phys Rev Lett* 78: 4446–4449